

# Stress Analysis of Rail Joint under Wheel Load

Sisay Guta<sup>1</sup>, Daniel Tilahun<sup>2</sup>

Ms. Student, School of Mechanical and Industrial Engineering, AAU technology institute, Addis Ababa, Ethiopia<sup>1</sup>

Assistant Professor, School of Mechanical and Industrial Engineering, AAU technology institute, Addis Ababa, Ethiopia<sup>2</sup>

**Abstract:** The main objective of this study is analysing and identifying the stresses on bolted rail joint due to the wheel load to predict and minimize failures caused. This studies use the hertz contact theory to perform the analysis for three various position of bolted rail joint on sleeper. This study covers only the stress and failure caused by the wheel load. The 3D model has done on modeling package of CATIAV5R16. Assembly model has created in assemble workbench of CATIA after individual component of joint had created on part work bench. The assembly of bolted rail joint contains rail, joint bars, bolts, nuts and washers. After the assembly is accomplished on CATIA, it was imported in to the ANSYS<sub>R14.5</sub> to analyze the stress caused by vertical load. ANSYS solves governing differential equations by breaking the problem into small elements. The wheel structure discretized using CONTA174 element. CONTA 170 three dimensional element is used to discretize rail. During the analysis of wheel/rail contact in ANSYS software, the parameters have been used axle load, angular velocity and gravitational acceleration. From ANSYS software simulation result when the rail joint between sleepers, the rail joint highly exposed to the equivalent, normal, shear stresses and contact pressure than the rest. For this reason, the service life of the rail joint between sleepers is small as compared to the remaining rail joint location. When the joint is on the sleeper, the stress on the rail joint is small in comparison to the rail joint between sleepers and rail joint approach to the sleeper, it will be better.

**Key word:** Rail Joint, Stress, Pressure, Sleeper, load

## I. INTRODUCTION

Rail is the most important track element subjected to wheel loads. It must be able to securely sustain these loads applied in vertical, lateral, and longitudinal directions and subsequently transfer them to the underlying supports. It is therefore very necessary, in particular from a safety point of view, to ensure the proper functioning of rails in the track system [3].

Rails are produce in fixed lengths and need to be joined end-to-end to make a continuous surface on which trains may run. There are essentially two different type of a rail joint.

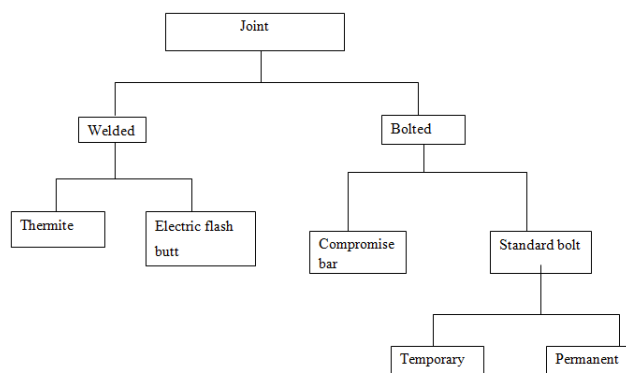


Figure 1: Rail Joint Classification.

The rail joints create discontinuities in the running surface of the rails. The joint parts of the rail have a lower vertical bending stiffness than the normal rail track. These discontinuities produce different type of static and

dynamic stresses on the running surface. These stresses on the rail head produce weakness on the joint and rail end. They cause different type of failures at the rail joint compare to the normal rail.

Based on other country experience, the following failures mode is at joint:-

- Delamination of end part of rail and joint bar.
- Broken joint bar and looseness of the bolt.
- Dislocation and deformation of the joint bar and rail.
- Fatigue wear of rail end due to repeated loading of a surface.
- Fretting damage on the joint parts and on rail due to the relative oscillatory movement of small amplitude that may occur between two contact surfaces subjected cyclic load.

The stress field created by the contact stresses was first introduced by Heinrick Hertz in 1881[4]. Assessment of contact stresses at the wheel–rail interface is one of the most important aspects of railway research, considering the many phenomena involved. For this reason, many scientists have approached the problem mainly by means of theoretical or numerical method.

Determine the size and stress distribution wheel –rail contact pressure using the ultrasonic reflection studied by Marshall [6]. 3D finite element analysis is used to study the effect of the discontinuity of the rail ends and the presence of lower modulus insulation material at the gap performed by Zong [10].

As it is mentioned on the above review, this part needed more research to improve the wearing rate, damage and failure of the rail joint component, to increase the comfort and safety of the passenger. This research contributes some additional discover by adding new methods on the existing knowledge.

This paper describes a similar approach with the previous one. However, it has two significant differences from the previous one. The paper begin neither focus on insulated rail joint nor insulated material in stain to study the stresses on standard (non- insulated) rail joint under vertical wheel load, then how to differ based on the three location of rail joint on sleepers. It is not only find the stress distribution, deflection and strain of joint under static wheel load but also it studies dynamic wheel load effect on the rail joint.

## II. MODEL AND ANALYSIS OF STRESS

There are many theories on the contact geometry. However, many published papers use the hertz theory to understand it easily. The hertz theory has been developing since 1881[4]. Hertzian contact theory, explain a relationship for determining the contact pressure distribution and contact area of a solid bodies while in contact with an elastic sphere or cylinder under an applied load. For this paper, hertz theory is much preferable than others theory. The analysis of the wheel/rail contact is covered by using the elliptical contact shape to solve the stress, pressure, and fatigue wear caused by the vertical load.

The wheel profile consists of a flange to guide the trains along the rails and a conical tread that contacts rail head, and rail has many curvatures to guide wheel properly. The contact positions of the wheel / rail are different in the different situation. However, this paper uses the contact between the wheels tread and rail head. The contact area between wheel and rail are very small compared to their dimension.

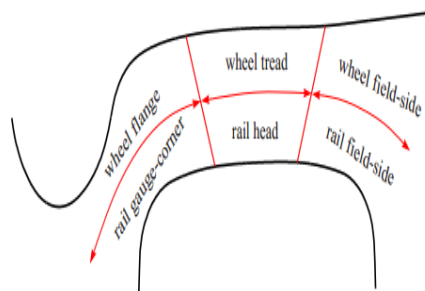


Figure 2: Contact Zone of Wheel/Rail.

### III. STRESS MODEL USING HERTZIAN THEORY

High stresses are inducing when a vertical load applied on the rail joint. This can cause serious problem on rail joint. Hertz developed a theory to calculate the contact area and stress between the two contact surfaces. The purpose of this paper is to focus on the hertz theory, when the wheel and rail contact occur 200mm form the end gap of the rail. As shown in the figure below the joint bars are connected at rail web, so that the wheel doesn't contact to the joint bar.

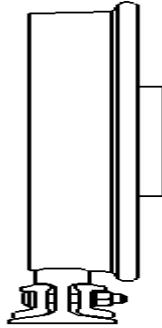


Figure 3: Wheel/Rail Contact at Rail Joint.

When two elastic non conforming bodies get together, according to the Hertz contact theory, the contact area is elliptical in shape with a major semi-axis “a” and a minor semi-axis “b” [22].

The contact pressure distribution in this area represents as semi-ellipsoid, which can be expressed as:

$$P(r) = p_o \sqrt{1 - \frac{x^2}{a^2} - \frac{y^2}{b^2}} \quad (1)$$

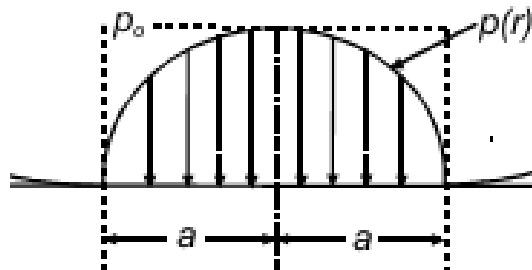


Figure 4: Pressure Distribution at Contact Zone [8].

From the above formula a and b are semi axes of the contact ellipse whereas x and y are the required coordinates to specify the point of contacts on the rail head based on the lateral rail surface parameter.

If  $x=0$  and  $y=0$ , the point of contact is on the centerline of the rail head the stress is maximum, which is equal to:

$$P = p_o, \text{ where } p_o = \frac{3F}{2\pi ab} \quad (2)$$

F is the vertical load act on the rail head

Based on the size and orientation of the contact, the positions of the contact point may be shifted in different directions based on the direction of x or y. However, based on Hertz contact formula and assumptions, the stress due to wheel/rail contact decreases and becomes zero when it goes far away from the centerline of the rail head.

Similarly, the wheel/rail contact stress is inversely proportional to the major and minor axis of the contact ellipse[20].

The contact area determined as follows:

$$a = m(3\pi F(\frac{K_w+K_r}{4K_3}))^{1/3} \quad (3)$$

$$b = n(3\pi F(\frac{K_w+K_r}{4K_3}))^{1/3} \quad (4)$$

m and n are Hertz coefficients and they are given as a function of the angle (0° -180°)

$$\theta = \cos^{-1} \frac{K_4}{K_3} \quad (5)$$

$\theta$  is rail curvature

$K_w$  and  $K_r$  are constants that depend on the material properties of railway wheel and rail respectively.

$$K_w = \frac{1-(\nu_w)^2}{\pi E_w} \quad (6)$$

$\nu_w$  and  $E_w$  are Poisson's ratio and young's modulus of the railway wheel material respectively.

$K_w$  is constants that depend on the material properties of railway wheel.

$$K_r = \frac{1-(\nu_r)^2}{\pi E_r} \quad (7)$$

$\nu_r$  and  $E_r$  are Poisson's ratio and young's modulus of rail material

$K_r$  is constants that depend on the material properties of rail.

$$K_3 = \frac{1}{2}(\frac{1}{R_{1w}} + \frac{1}{R_{2w}} + \frac{1}{R_{1r}} + \frac{1}{R_{2r}}) \quad (8)$$

$$K_4 = \frac{1}{2} \left( (\frac{1}{R_{1w}} - \frac{1}{R_{2w}})^2 + (\frac{1}{R_{1r}} + \frac{1}{R_{2r}})^2 + 2 \left( \frac{1}{R_{1w}} - \frac{1}{R_{2w}} \right) \left( \frac{1}{R_{1r}} - \frac{1}{R_{2r}} \right) \cos 2\varphi \right)^{1/2} \quad (9)$$

$K_3$  and  $K_4$  are depends on the geometric propeties of the two bodies.

$R_{1w}$  and  $R_{1r}$  are the principal rolling radii of the wheel and rail respectively.

$R_{2w}$  and  $R_{2r}$  are the principal transverse radii of curvature of the wheel and radii respectively.

$\varphi$  is straight curvature of the rail.

The direction of the axes of the contact ellipse can be determined based on the radii of curvature and the rolling radii for the two bodies in contact.

If  $\frac{1}{R_{1w}} + \frac{1}{R_{2w}} \geq \frac{1}{R_{1r}} + \frac{1}{R_{2r}}$  : the transverse semi axis of the contact ellipse (y direction) is greater than or equal to the longitudinal semi-axixs.

If  $\frac{1}{R_{1w}} + \frac{1}{R_{2w}} \leq \frac{1}{R_{1r}} + \frac{1}{R_{2r}}$  : the transverse semi axis of the contact ellipse (y direction) is less than or equal to the longitudinal semi-axis.

#### IV. FINITE ELEMENT THEORY FOR CONTACT BODY

Finite element theory is used to show that relationship among the contact force, applied force, support and free displacement of wheel /rail contact. During the formulations of finite element the contact between the wheel and rail is assumed:

- Isotropic
- Homogeneous
- Linear elastic body  $\Omega$  with boundary conditions

The linear elastic bodies have four boundaries condition as shown in the figure below.

- $\Gamma_1$  is the boundary with zero displacement.
- $\Gamma_2$  is the boundary where measured displacements.
- $\Gamma_3$  is the boundary with unknown contact forces  $F_c$  and unknown contact deformation or displacements.
- $\Gamma_4$  is the boundary where applied forces  $F_a$  and the other are free surface except those mentioned above. The displacements on boundary  $\Gamma_4$  are unknown.

Let's recall the general form of static finite element system, which is

$$KU=F \quad [5] \quad (10)$$

K, U and F are stiffness matrix of the system, nodal vector displacement, and nodal vector forces. According to the classification of the boundary, it constructs the finite element equation in the following form:

$$\begin{pmatrix} K_{11} & K_{12} & K_{13} & K_{14} \\ K_{21} & K_{22} & K_{23} & K_{24} \\ K_{31} & K_{32} & K_{33} & K_{34} \\ K_{41} & K_{42} & K_{43} & K_{44} \end{pmatrix} \begin{pmatrix} U_1 \\ U_2 \\ U_3 \\ U_4 \end{pmatrix} = \begin{pmatrix} F_1 \\ F_2 \\ F_3 \\ F_4 \end{pmatrix} \quad (11)$$

$K_{ij}$  and  $F_1$  are sub-stiffness matrix and vector of reaction forces on the boundary  $\Gamma_1$ .

$F_2$  is a vector forces on the boundary  $\Gamma_2$  with measured displacements, usually there is no force on the measured boundary.

$F_c$  and  $F_a$  are vector of unknown reaction or contact forces on the boundary  $\Gamma_3$  and vector of known applied forces on the boundary  $\Gamma_4$ .

$U_1$  and  $U_2$  are known displacements on constrained boundary  $\Gamma_1$  and measured displacement on free boundary  $\Gamma_2$

$U_3$  and  $U_4$  are unknown displacements on contact boundary  $\Gamma_3$  and unknown displacements on boundary  $\Gamma_4$  with known applied force  $F_a$ , the free surface with no applied force and the internal nodes where net force is zero.

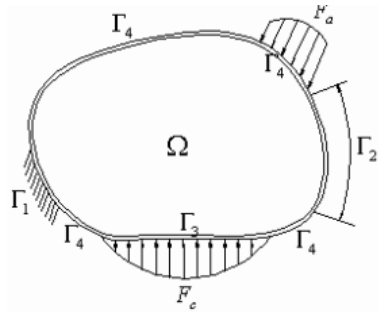


Figure 5: Contact Model Analyze [21].

The stiffness matrix is singular and no unique solution for displacement is possible if the structure is unsupported for the above structure stiffness equation. For this reason all displacement on the boundary  $\Gamma_1$  are zero, that means  $U_1=0$ . When apply this condition to the system matrix and vector in equation 10 FEA equation becomes:

$$\begin{bmatrix} K_{22} & K_{23} & K_{24} \\ K_{32} & K_{33} & K_{34} \\ K_{42} & K_{43} & K_{44} \end{bmatrix} \begin{bmatrix} U_2 \\ U_3 \\ U_4 \end{bmatrix} = \begin{bmatrix} F_2 \\ F_c \\ F_a \end{bmatrix} \quad (12)$$

To calculate the contact forces  $F_c$  at  $U_2$ . Multiple 3<sup>rd</sup> row of the stiffness matrix with displacement matrix, then equation became:

$$K_{42}U_2 + K_{43}U_3 + K_{44}U_4 = F_a \quad (13)$$

$$U_4 = K_{44}^{-1}[F_a - K_{42}U_2 - K_{43}U_3] \quad (14)$$

Multiple the 2<sup>nd</sup> rows with displacement column, the equation became;

$$K_{32}U_2 + K_{33}U_3 + K_{34}U_4 = F_c \quad (15)$$

$$U_3 = K_{33}^{-1}[F_c - K_{32}U_2 - K_{34}U_4] \quad (16)$$

When equation 3.13 substitute in the equation 3.14,  $U_3$  became;

$$U_3 = K_{33}^{-1}[F_c - (K_{33} - K_{34}K_{44}^{-1}K_{43})U_2 - K_{34}K_{44}^{-1}F_a + K_{34}K_{44}^{-1}K_{43}U_3] \quad (17)$$

Therefore the displacement at the contact point is:

$$U_3 = K_{33}^{-1}[F_c - (K_{33} - K_{34}K_{44}^{-1}K_{43})U_2 - K_{34}K_{44}^{-1}F_a + K_{34}K_{44}^{-1}K_{43}U_3] \quad (18)$$

Generally, the contact between the wheel and rail are considered to determining the failure effect of rail end and rail joint.

Stress -strain relationship of structural analysis

$$\{\sigma\} = \{K\} \{\epsilon^{el}\} \quad (19)$$

$\epsilon^{el}$ ,  $\sigma$  and  $D$  are elastic strain vector, stress vector and elastic stiffness matrix.

$$\{\sigma\} = \{\sigma_x, \sigma_y, \sigma_z, \sigma_{xy}, \sigma_{yz}, \text{ and } \sigma_{xz}\} \quad (20)$$

$$\{\epsilon^{el}\} = \{\epsilon\} - \{\epsilon\}^th$$

$$\{\epsilon\} = \{\epsilon\}^th + \{D^{-1}\} \{\sigma\} \quad (21)$$

$$\{D^{-1}\} = \begin{bmatrix} 1/E_x & -\nu_{xy}/E_x & -\nu_{zy}/E_x & 0 & 0 & 0 \\ -\nu_{yx}/E_x & 1/E_x & -\nu_{yz}/E_x & 0 & 0 & 0 \\ -\nu_{zx}/E_x & -\nu_{zy}/E_x & 1/E_x & 0 & 0 & 0 \\ 0 & 0 & 0 & 1/G_{xy} & 0 & 0 \\ 0 & 0 & 0 & 0 & 1/G_{yz} & 0 \\ 0 & 0 & 0 & 0 & 0 & 1/G_{zx} \end{bmatrix}$$

$E_x$  and  $G_{xy}$  are young's modulus in the x direction and shear modulus in the xy plane

$\nu_{xy}$  and  $\nu_{yx}$  are major poisson's ratio and minor poisson's

Also the  $\{D^{-1}\}$  matrix is presumed to be symmetric, so that

$$\frac{\nu_{xy}}{E_y} = \frac{\nu_{yx}}{E_x}$$

$$\frac{\nu_{zx}}{E_z} = \frac{\nu_{xz}}{E_x}$$

$$\frac{\nu_{zy}}{E_z} = \frac{\nu_{yz}}{E_x}$$

$$\frac{\nu_{zx}}{E_z} = \frac{\nu_{xz}}{E_x}$$

$$\frac{\nu_{zy}}{E_z} = \frac{\nu_{yz}}{E_y}$$

The element integration point strain and stress are:

$$\{\epsilon^{el}\} = \{B\}\{U\} - \{\epsilon\}^{th}, \text{ for this case, } \{\epsilon\}^{th} \text{ is zero}$$

$$\{\sigma\} = \{D\}\{\epsilon^{el}\}$$

$B$  and  $\{\epsilon\}^{th}$  are strain - displacement matrix evaluated at integration point and thermal strain

$\epsilon^{el}$  is strain that cause stress

Maximum stress failure criteria

$$\epsilon_x = \text{maximum of } = \begin{cases} \frac{\sigma_{yc}}{\sigma_{yc}^f}, \frac{\sigma_{xy}}{\sigma_{xy}^f} \\ \frac{\sigma_{yc}}{\sigma_{yc}^f}, \frac{\sigma_{yz}}{\sigma_{yz}^f} \\ \frac{\sigma_{zc}}{\sigma_{zc}^f}, \frac{\sigma_{zx}}{\sigma_{zx}^f} \end{cases} \quad (22)$$

$\sigma_x$ ,  $\sigma_y$  and  $\sigma_z$  are stress in x, y, z direction.

$\sigma_{xc}^f$ ,  $\sigma_{yc}^f$  and  $\sigma_z$  are normal stress failure in x, y, z direction.

$\sigma_{xy}$ ,  $\sigma_{xy}$  and  $\sigma_{xy}$  are shear failure in xy, yz, xz direction.

## V. RAIL SUPPORT

Railway system uses sleeper to provide a support and transmit the vertical, lateral and longitudinal load from the rail down to ballast bed.

In this paper, there are three location of rail joint selected to perform the analysis based on straight rail way line. The space between two sleepers is 625mm.

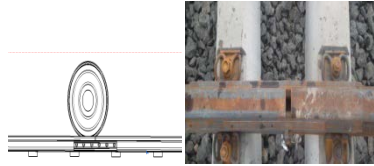


Figure 6: Rail Joint at the Center of Two Sleepers (a) 3D model (b) Addis Ababa LRT track.

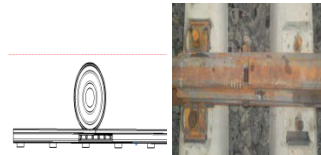


Figure 7: Rail Joint Approach to Sleeper (a) 3D Model (b) Addis Ababa LRT track

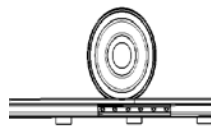


Figure 8: Rail Joint on Sleeper.

## VI. WHEEL/RAIL CONTACT SIMULATION

As discuss on above portion, rail joint is a critical component of the railway track infrastructure. For this reason, it needs careful analysis to protect the rail joint. Standard bolted joint contains rail, joint bars, bolts, nuts and washers are used to secure fastening assembly. The assembly is done on the modeling package of CATIAV5R16. CATIAV5R16 is 3D mechanical design software for creating 3D prototypes, used to design, visualize and simulate of the analysis.



Figure 9: Three Dimensional Model of Wheel/Rail at Rail Joint.

Assembly model created in assemble workbench of the CATIA after each component of joints created on part of work bench. The assembly model consists; rails, joint plates, bolts, nut, washer, and wheel. The dimensions and specifications of each part are, based on the relevant standard.

#### Dimensions and Specification

Type of rails for main lines and depot = 50 kg/m

Track gauge = 1435

Wheel diameter (new wheel) =  $\leq 660$  mm

Plate length=820 mm

Plate thickness = 19 mm

Sleeper space =625 mm

End gap = 5 mm

Joint bar bolt and nut = M28 (AT109)

Spring washer =  $\Phi 34$ mm

## VII. FINITE ELEMENT MODELING

Finite element method is used to analyze the response of the rail joint to the static and dynamic load. The FE analysis is performed using structural analysis of the ANSYS R14.5 work bench software after imported 3D assemblies form CATIA software.

ANSYS is a general purpose finite element of modeling package for numerical solved problems. Like any finite element software, ANSYS solves governing differential equations by breaking the problem into small elements. When the wheel is contact element and the rail is target element, the wheel and rail will be different. The wheel structure discretized using CONTA174 element. CONTA 170 three dimensional elements are used to discretize rail.

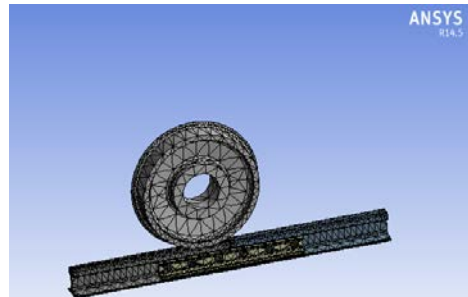


Figure 10: Mesh of Assembled Part on ANSYS Workbench.

The contact point of wheel and rail are used fine mesh to make the solution accurate.

#### Material Selection of rail joint component

Poisson's Ratio = 0.3

Young's modulus (MPa) = 207MPa

Ultimate tensile strength MPa = 780MPa

Yield strength = 640MPa

Density = 7800kg/m

Elongation =12%

### VIII. LOAD AND SUPPORT

All material properties and data are used based on Ethiopia Railway Corporation. Vertically downward load is sum of 3% allowance, maximum axle load. The overall load is the sum of the total tram weight and carrying capacity of the vehicle. The overall load is classified to each axle of the vehicle then the axle load is classified to each wheel vehicle. Carrying capacity of vehicle has calculated by take average of 60kg/ person and the total rate of passenger inside of the tramcar is 317. 70 km/h is the maximum operating speed of vehicle.

The total vertical load is calculated as follows:

- a. Tram car weight = 44 ton
  - The load apply on each axle = 7.333 ton = 73333N
  - The load apply on each wheel = 3.667 ton = 36667 N
- b. Carrying Capacity = 60kg/person \*317 person = 19020N
- c. Over all capacity = Tram car weight on each wheel + Carrying Capacity
- d. Maximum Axle load =  $11,0000 \text{ kg} \times 9.81\text{m/s}$   
=107,710N
- e. The total vertical load = maximum Axle load +3% maximum Axle load  
  
= 111147.3N
- f. The load on each wheel = 55573.63N

Note: The maximum axle load is taken to perform the analysis

The maximum parameter is used to perform the analysis. Material properties of the rail, wheel and plate are assumed the same for the simplicity of the problem.

In order to attain the accurate stress analysis for any application, the support and the load must be defined. This will ensure that the solution incorporates to support of the domain. The place where the sleepers contact the rail considered as fixed support.

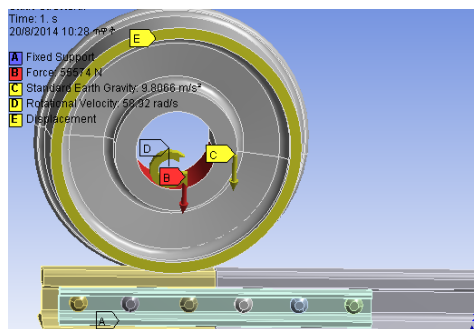


Figure 11: Load applied.

## IX. SIMULATION RESULTS

The analysis is performed by using finite element model consists of the static analysis to determine the impact of the wheel load. Different support location is used to perform finite element analyses, although the geometry and load application are the same for all support location.

### I. Stress

Stress is defined as the average force per unit area that some particle of a body exerts on an adjacent particle, across an imaginary surface that separates them.

Case 1: When the rail joint on the sleeper.

#### A. Equivalent (von- mises) stress(Pa)

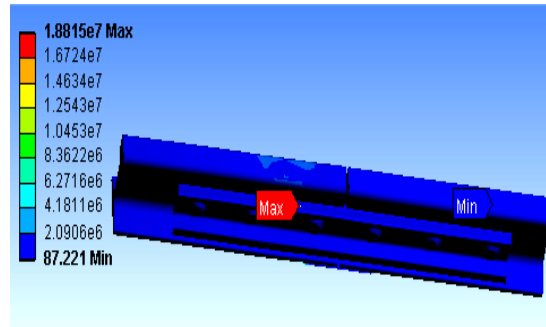


Figure 12: Von-Mises Stress When Rail Joint on the Sleeper.

As shown in above figure, the maximum von-Mises stress is 18.82MPa and the minimum von –mises stress is 87.22Pa, when rail joint on the sleeper.

#### B. Normal stress(bending stress)(Pa)

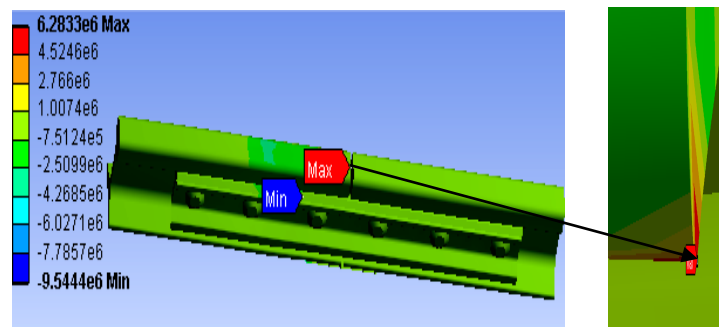


Figure 13: Normal Stress When Rail Joint on the Sleeper.

As shown in above figure, the maximum normal stress is 6.28MPa and the minimum normal stress is -9.55MPa, when the rail joint on the sleeper.

#### C. Shear stress(Pa)

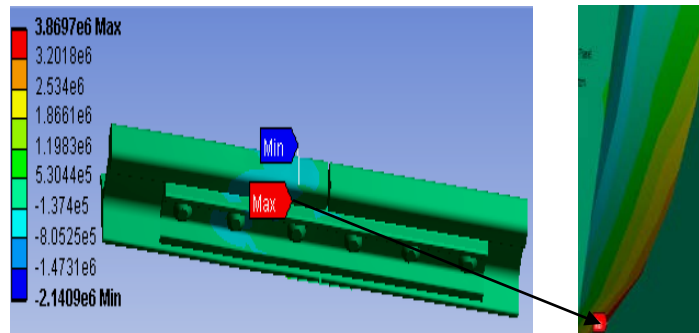


Figure 14: Shear Stress When Rail Joint on the Sleeper.

As shown in above figure, the maximum shear stress is 3.87MPa and the minimum shear stress is -2.14MPa, when the rail joint on the sleeper.

Case 2: When rail joint approach to sleeper.

A. Equivalent stress (von –mises stress) (Pa)

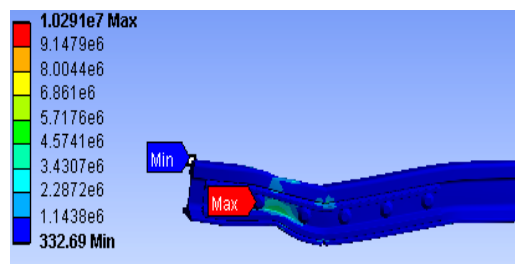


Figure 15: Von - Mises Stress When Joint Approach to Sleeper Rail.

As shown in above figure, the maximum von mises stress is 10.29MPa and the minimum von mises stress is 332.69Pa, when rail joint approach to sleeper.

B. Normal stress (bending stress)(Pa)

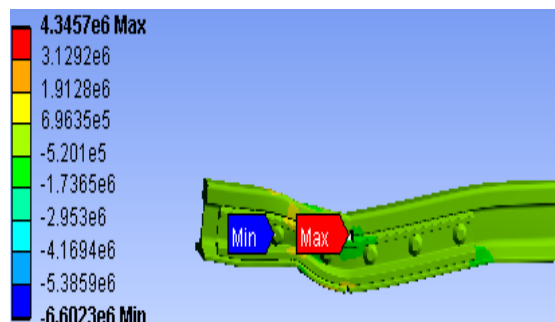


Figure 16: Normal Stress When Rail Joint Approach to The Sleeper

As shown in above figure, the maximum normal stress is 4.35MPa and the minimum normal stress is -6.6MPa, when rail joint approach to the sleeper.

C. Shear stress (Pa)

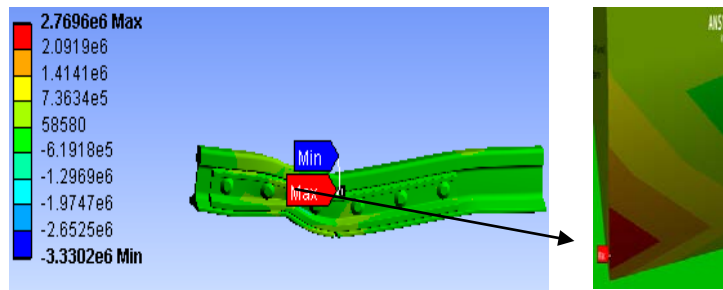


Figure 17: Shear Stress When Rail Joint Approach to the Sleeper.

As shown in above figure, the maximum shear stress is 2.77MPa and the minimum shear stress is -3.33MPa, when the rail joint on the sleeper.

Case 3: When the rail joint between sleepers

A. Equivalent stress(von mises stress)(pa)

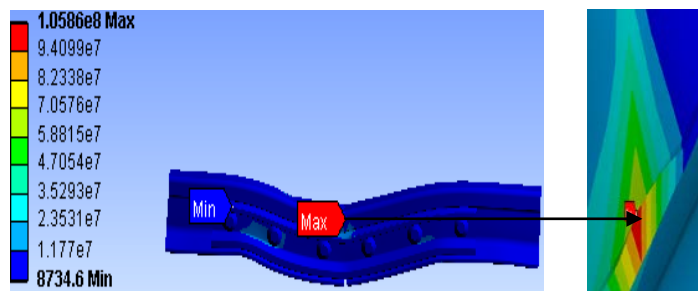


Figure 18: Von Mises Stress When Rail Joint between the Sleepers.

As shown in above figure, the maximum von mises stress is 105.9MPa and the minimum von mises stress is 8734.6Pa, when rail joint between the sleepers.

B. Normal stress (bending stress)(pa)

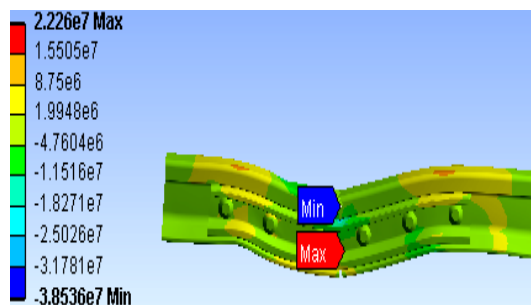


Figure 19: Normal Stress When Rail Joint between the Sleepers

As shown in above figure, the maximum normal stress is 22.3MPa and the minimum normal stress is -38.5MPa, when rail joint between the sleepers.

C. Shear stress

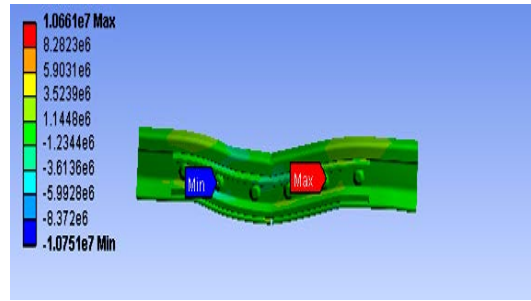


Figure 20: shear stress when rail joint between the sleepers

As shown in above figure, the maximum shear stress is 10.66MPa and the minimum shear stress is -10.75MPa, when rail joint between the sleepers.

II. Pressure

Case 1: When rail joint on the sleeper.

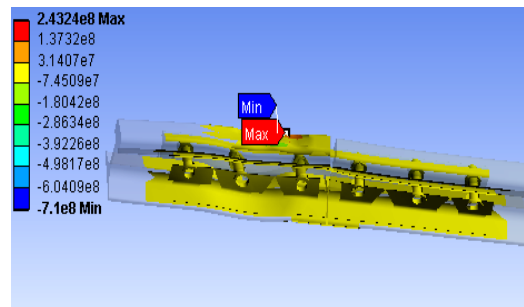


Figure 21: pressure distribution when rail joint on the sleeper.

As shown in above figure, the maximum pressure is 243.2MPa and the minimum pressure is -710MPa, when rail joint on the sleeper.

Case 2: When rail joint approach to the sleepers.

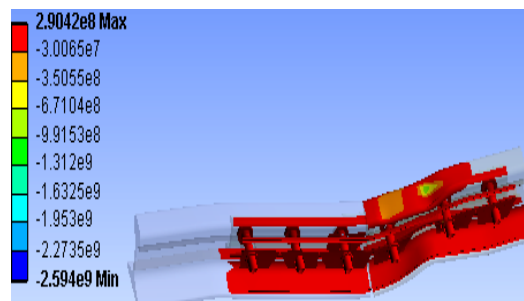


Figure 22: pressure distribution when joint approach to the sleepers.

As shown in above figure, the maximum pressure is 290.4MPa and the minimum pressure is -2594MPa, when rail joint approach to the sleeper.

Case 3: When rail joint between the sleepers.

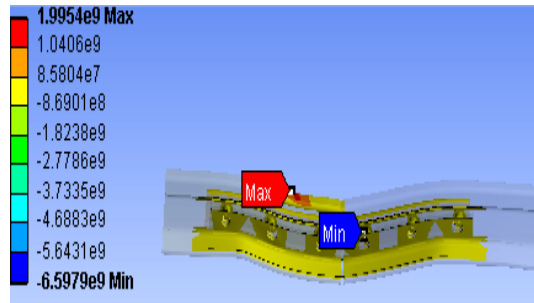


Figure 23: pressure distribution when rail joint between the sleepers.

As shown in above figure, the maximum pressure is 1995.4MPa and the minimum pressure is -6597.9MPa, when rail joint between the sleepers.

### III. Fatigue Stress

Case 1: When rail joint on the sleeper.

A. Biaxiality indication

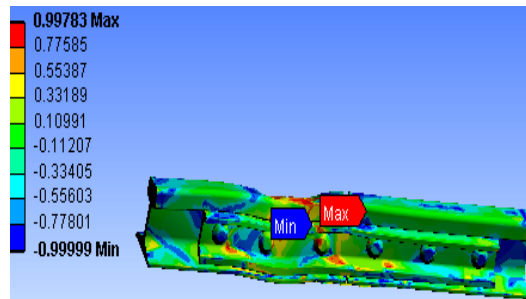


Figure 24: Biaxiality Indication When Rail Joint on the Sleeper.

As shown in above figure, the maximum biaxial indication is 0.9997 and the minimum biaxial induction is -0.999, when rail joint on the sleeper.

B. Factor of safety

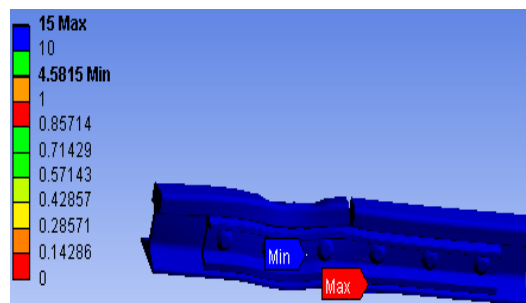


Figure 25: safety factor when rail joint on the sleepers.

As shown in above figure, the maximum safety factor is 15 and the minimum safety factor is 0.1428, when rail joint on the sleeper.

Case 2: When rail joint approach to the sleeper.

A. Biaxiality indication

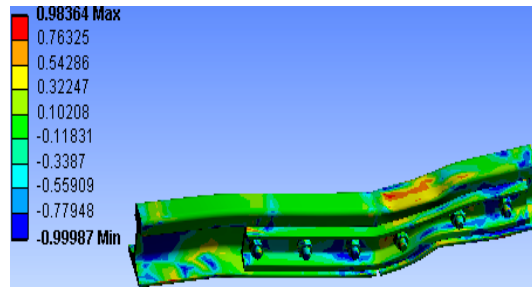


Figure 26: Stress Distribution When Rail Joint Approach to the Sleeper.

As shown in above figure, the maximum biaxial indication is 0.9836 and the minimum biaxial induction is -0.9998, when rail joint approach to the sleeper.

B. Factor of safety

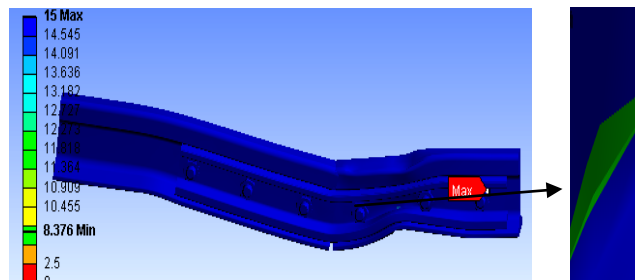


Figure 27: Safety Factor When Rail Joint Approach to the Sleeper.

As shown in above figure, the maximum safety factor is 15 and the minimum safety factor is 2, when rail joint approach to the sleeper.

Case 3: When rail joint between the sleepers

As shown in above figure, the maximum alternating stress is 10.59MPa and the minimum alternating stress is 8734.6Pa, when rail joint between the sleepers.

A. Biaxially indication

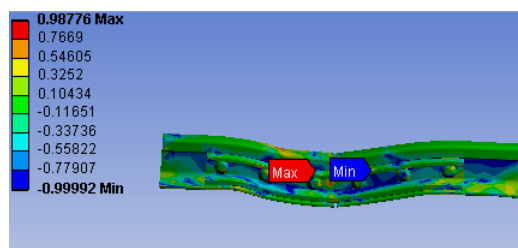


Figure 28: Biaxial Induction When Rail Joint between the Sleepers.

As shown in above figure, the maximum biaxial indication is 0.9836 and the minimum biaxial induction is -0.9998, when rail joint between the sleepers.

## B. Factor of safety

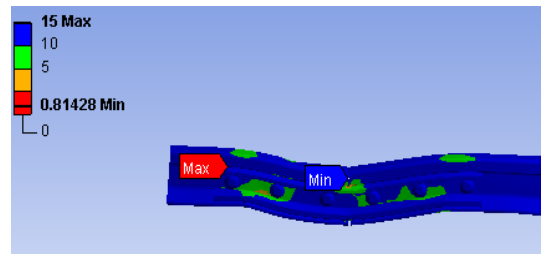


Figure 29: Safety Factor When Rail Joint between the Sleepers.

## X. CONCLUSION

In this study, the responses of a bolted rail joint component are determined under static and dynamic loads, the results are assumed to be significant. The analysis can include stress, strain and fatigue responses of bolted rail joint caused by vertical wheel load. The analysis is taking into account by using various position of bolted rail joint on the sleepers.

From the results obtained in the static and dynamic analysis, the three cases have different stress distribution on rail joint. The stress distribution when the rail joint between sleepers is high in comparison to rail joint approach to sleeper and rail joint on sleeper. The stress distribution is when the joint on sleeper is small in comparison to the remaining.

This part of rail track needed more attention than other parts, to reduce the problem related to the rail joint. This paper recommends using the sleeper during the rail joint position. This paper is also recommend, the bolt around the end gap need more strength than part of the joint due to the exposure of the vertical load. In addition to this the end rail is seen in static and dynamic result, it is needed a special treatment to reduce the rail head wear rate.

## XI. ACKNOWLEDGMENT

I would like to express my deepest pleasure and gratitude to my advisor Dr .Daniel Tilahun for his countless good advice, valuable guidance and continuous encouragement throughout this study. I would also like to thank my co-advisor Ato Habtamu Tekubet for his help with support, valuable suggestions and discussions that he has provided me during this research.

My special thanks go to Araya Abera PhD candidate who was always willing to help and to share his experience about ANSYS soft ware.

I would like to thank my entire friends who have contributed to my education and have supported me through my graduate study. I would like to express my deepest gratitude to my friend Meseret Tesfaye who has been so giving his hand though out my entire study and especially for taking the pressure off my shoulders when it mount up.

I am also grateful to my friend Zelalem Motbanor for carefully reading my reports given valuable suggestion on it.

Finally I wish to express sincere thanks to my family for their good support, patience and understanding while preparing this thesis.

## REFERENCE

1. Michelangelo Bozzone, "Dynamic Analysis of Railway Systems Using Computationally Efficient Wheel-Rail Contact Models", Università degli studi di roma, 2009/2010.
2. Coenraad Esveld, "Modern Railway Track", 2nd edition, MRT production, 1-660, 2001.
3. Parsons Brinckerhoff, "Track Design Handbook for Light Rail Transit", Second Edition, National Academy of Sciences, Washington, d.c. 2012.
4. W. Yan and F. D. Fischer, "Applicability of the Hertz contact theory to rail-wheel contact problems", *Archive of Applied Mechanics* 70 (2000) 255±268.
5. Johnson K. L, "Contact Mechanics", (Cambridge University Press, Cambridge), 1985.
6. M.B. Marshall, R.Lewis, R.S. Dwyer-Joyce, O. Olofsson, S. Björklund, "Measuring Wheel/Rail Contact Stresses using Ultrasound", 14th International Wheel set Congress, October 2004
7. T.X WU and D.J .Thompson, "Theoretical Investigations of Wheel/Rail Non –Liner Interaction Due to Roughness Excitation", ISVR Technical Memorandum .no852, 1-39, August 2000.
8. RS Owyer- Joyce, "Tribological Design Data, The tribology Group of The Institution of Mechanical Engineers", 1st edition June 1997.
9. [www.atlantictrack.com](http://www.atlantictrack.com)
10. Nannan Zong and Manicka Dhanasekar, "Analysis of Rail Ends under Wheel Contact Loading", *International Journal of Mechanical and Aerospace Engineering* 6, 452-460, 2012.
11. Muhammad Akhtar, David Davis, Luis Maal Jeff Gordon and David Jeong, "Effects Of Track Parameters on Rail Joint Bar Stresses and Crack Growth", AREMA Annual Conference and Exposition Orlando, Florida, 2010.
12. Sunil Patel, Veerendra Kumar and Raji Nareliya, "Fatigue Analysis of Rail Joint Using Finite Element Method", vol2, ISSN2319-1163, Jan 2013.
13. Nirmal Kumar Mandal and Brendan Peach, "An Engineering Analysis of Insulated Rail Joints", *International journal of engineering science and technology*, vol2,2(8),3964-3988, 2010.
14. Nicolae Faur , Ion Goia , LaurenŃiu Culea, Anghel Cernescu and Assistent Radu Negru, "Stress-Strain Analysis For the Wheel-Rail Track Assembly at Urban Passenger Transport", 5th Int. Conference Structural Integrity of Welded Structures (ISCS2007), Timisoara, Romania, 20-21, Nov 2007.
15. Hiroo KATAOKA, Noritsugi ABE and Osamu Wakatsuk" Evaluation of Service Life of Jointed Rails, Track Structure & Component Group" Railway Technical Research Institute, Japan.
16. Anne K. Himebaugh, "Finite Element Analysis of Insulated Railroad Joints", Master of Science In Civil Engineering, 1-75 November 28, 2006.
17. Daniel Peltier, Christopher P. L. Barkan, Engineering Steven Downing and Darrell Socie, "Measuring Degradation of Bonded Insulated Rail Joints" , University of Illinois at Urbana-Champaign Urbana, IL 61801.
18. Zachary I. Charlton, " Innovative Design Concepts for Insulated Joints", Master of Science, Blacksburg, Virginia April 10, 2007.
19. Brandon Talamini , David and Y. Jeong, "Estimation of the Fatigue Life of Railroad Joint Bars", 2007 ASME/IEEE Joint Rail Conference & Internal Combustion Engine Spring Technical Conference, 1-10, March 13-16, 2007.
20. Addisu Negash, "Analysis of Wheel/Rail Contact Geometry and Applied Load Conditions on the Rail Head Surface", Addis Ababa university, Addis Ababa Ethiopian, October 2012.
21. Jiangtao Song and Randy J Gu, " A Finite Element Based Methodology for Inverse Problem of Determining Contact Forces Using Measured Displacements", *International Conference on Engineering Optimization* 01 - 05 June 2008.
22. Rogerb and Enblom, "On simulation of uniform wear and profile in the wheel –rail contact", doctoral thesis in railway technology ,Stockholm Publisher: KTH, ISSN 1651-7660/2006.
23. J. Sadeghi1 and P. Barati1, " Evaluation of conventional methods in Analysis and Design of Railway Track System", *International Journal of Civil Engineering*. Vol. 8, No. 1, 44-56, March 2010.
24. Radu Negru, Liviu Marsavina, Nicolae Faur, Cristiana Căplescu, "Analysis and Design of Adhesive-Bonded Corner Joints", 11. 5th Int. Conference Structural Integrity of Welded Structures (ISCS2007), Timisoara, Romania, 20-21 Nov 2007.
25. Radu Negru, Liviu Marsavina, Nicolae Faur, Cristiana Căplescu, "Analysis and Design of Adhesive-Bonded Corner Joints", 11. 5th Int. Conference Structural Integrity of Welded Structures (ISCS2007), Timisoara, Romania, 20-21, Nov 2007.
26. R.G. Fata, J.A. Jones, A.B. Perlman, and O. Orringer, " A Numerical Model for Estimation of Temperature-Time History and Residual Stress In Head-Hardened Rails", *Mechanical Engineering Department, Tufts University, Medford, MA 02155*, 495-7466.
27. M.A.Van, : Buckling Analysis of Continuous Welded Rail Track, HERO, vol4.43, 175-186, 1996.